JPPIPA 9(11) (2023)

Jurnal Penelitian Pendidikan IPA

Journal of Research in Science Education

http://jppipa.unram.ac.id/index.php/jppipa/index

Manufacture and Characterization of PVA-Enzyme/GA/PANI-HCl or PANI-p-toluentsulfonate/PVC-KTpClPB-o-NPOE Indicator Electrode Membranes, Analysis, XRD, SEM-EDX and FTIR

Abd Hakim S[1*]

[1] Department of Physics, Faculty of Mathematics and Natural Sciences, Universitas Negeri Medan, Medan, Indonesia.

Received: August 18, 2023
Revised: October 22, 2023
Accepted: November 25, 2023
Published: November 30, 2023

Corresponding Author:
Abd Hakim S
abdhakims@unimed.ac.id

DOI: 10.29303/jppipa.v9i11.5638

Abstract: This research aims at the synthesis and characterization of indicator electrode membranes consisting of PVA-Enzyme/GA/PANI/PVC-KTpClPB-o-NPOE, urea analyte. PANI-HCl and PANI-p-toluensulfonate conducting polymers, 61% and 66% o-NPOE plasticizer variations in PVC-KTpClPB, as well as urease enzyme activity in one or three drops of 0.5 mL PVA (50% water: 50% ethanol). The biosensor potentiometric method was used with the technique of immobilizing the urea enzyme which is the urea analyte. The multi-membrane indicator electrode is PVA-Enzyme/GA/PANI/PVC-KTpClPB-o-NPOE, PANI dissolved in HCl and p-toluensulfonic acid respectively at a concentration of 6 M and 2 M. Each membrane on the indicator electrode is coated with one time. Results of XRD analysis of the spectrum pattern of the PANI-HCl indicator electrode with intensities of 4400 a.u, 1386 a.u, 1724 a.u with a 2theta angle of 28.6 degrees, PANI-p-toluensulfonate with intensities of 10940 a.u, 9194 a.u, 5312 a.u with a 2theta angle of 18.2 degrees. SEM-EDX analysis showed differences in the morphology of the o-NPOE plasticizer of 61% and 66% as well as an increase in cps/eV from the number of drops of the urease enzyme, one drop was lower than three drops. FTIR analysis shows an increase in transmittance by PANI towards PPy. Analysis of the properties of a multi-membrane indicator electrode with one layer of the best sample is PANI-p-toluensulfonate.

Keywords: Elektroda indicator; HCl; Multi membrane; PVA-Enzim/GA/PANI/PVC-KTpClPB-o-NPOE; p-toluensulfonat

Introduction

This electrode has four layers, the first layer is urease enzyme immobilization, the second layer is GA cross-linking, the third layer is PANI conducting polymer with hydrochloric acid and p-toluensulfonic acid. H2SO4 has stronger electrolyte properties than HCl. P-toluensulfonic acid is stronger than HCl. Hydrochloric acid (HCl) is commonly used to clean metal surfaces. Immobilization of the urease enzyme is differentiated according to the number of drops of 0.5 mL of urease enzyme (50% water and 50% alcohol) in the PVA solution. GA cross-linking is best at 2.9%. Sulfuric acid in the PPy conducting polymer in the third layer of the indicator electrode. The results of the XRD analysis can be seen in Figure 4. The intensity against the 2theta diffraction angle. Hydrochloric acid and p-toluent in the PANI conducting polymer in the third layer of the indicator electrode were analyzed by XRD, as can be seen in Figures 5 and 6, respectively.

The acidic properties of H2SO4, p-toluent and HCl are sequentially stronger. Sulfuric acid is a strong mineral (inorganic) acid. P-toluenesulfonic acid or abbreviated as TsOH, is an organic compound that has the formula CH3C6H4SO3H. It is a white solid that is soluble in water, alcohol, and other polar organic

How to Cite:
Hakim S, A. (2023). Manufacture and Characterization of PVA-Enzyme/GA/PANI-HCl or PANI-p-toluentsulfonate/PVC-KTpClPB-o-NPOE Indicator Electrode Membranes, Analysis, XRD, SEM-EDX and FTIR. *Jurnal Penelitian Pendidikan IPA*, *9*(11), 10043–10050. https://doi.org/10.29303/jppipa.v9i11.5638

solvents. A powerful organic acid, one million times stronger than benzoic acid. Hydrochloric acid with the chemical formula HCl is a strong acid that is very corrosive. HCl is usually used in industry for iron purification and also for cleaning equipment. According to figures 4, 5 and 6, it turns out that the nature of the acid affects the intensity of the 2theta diffraction angle. The H2SO4 sulfuric acid in the PPy conduction polymer is lower in intensity than hydrochloric acid and p-toluensulfonic acid in the PANI conduction polymer. So it is true that the PPy conducting polymer is weaker than the PANI conducting polymer.

There is a change in activity in the conducting polymer PPy with the strong acid H2SO4 8M according to XRD analysis table 1. The intensity of H2SO4-1 224 a.u, H2SO4-3 236 a.u reflects the conduction properties and the 2theta diffraction angle of around 44 degrees reflects the activity. PANI conducting polymer with hydrochloric acid HCl intensity 4400 a.u sample S2, 1902 a.u sample S5, 2652 a.u sample S7 2theta diffraction angle of about 28 degrees. PANI conducting polymer with p-toluensulfonate intensity 10940 a.u sample S3, 9194 a.u sample S6, 5312 a.u sample S8, diffraction angle 2theta about 18 degrees. Not only does cross-linking GA increase conductivity (Hsu et al., 2022), conducting polymers with high conductivity, large surface area, and improved electron transfer kinetics, increase the electrocatalytic activity of sensors (Terán-Alcocer et al., 2021).

On the basis of (Elbehery et al., 2019; Hakim S, 2022; Kaur et al., 2017) the indicator electrode is made of four layers, one layer each with o-NPOE variations of 61% (Hakim S, 2022) and 66% (Vlascici et al., 2008).

Method

Urase enzyme electrode membrane 6 mg 10 mL (50% water : 50% alcohol). PVA : PVC 1:1, namely 35 mg : 35 mg. Lipophilic cationic derivative (KTpClPB): PVC = 2:1, namely 50 mg : 35 mg (Vlascici et al., 2008). PVC (Poly vinyl chloride) (Kaur et al., 2017) consists of a plasticizer, o-nitrophenyloctylether (o-NPOE), lipophilic salts, and sodium tetraphenylborate (NaTPB), and a number of ionophores. Plasticizer o-nitrophenyloctylether (o-NPOE) (Kaur et al., 2017) 61% (Hakim S, 2022) and 66% (Vlascici et al., 2008).

The tungsten indicator electrode is coated with PVA-Enzyme/GA/PANI-hydrochloric acid, p-toluensulfonate/PVC-KTpClPB-o-NPOE. Materials purchased at Sigma-Aldrich were tungsten with a diameter of 1.0 mm 99.99% Aldrich 267562, PVA[-CH2CHOH-]n, enzyme EC 3.5.1.5 (Urease) U4002, 50 - 100 ku type ix, glutaraldehyde (GA) , PVC (CH2CHCl)n, potassium tetrakis (4-chlorophenyl) borate (KTClPB), o-nitrophenyloctylether (o-NPOE), Tetrahydrofuran C4H8O; Phosphate Buffer KH2PO4, KCl, urea standard 56180, from Sigma-Aldrich. The potentiometer cell is equipped with an Ag/AgCl MF-2052 RE-5B reference electrode with an indicator electrode PVA-Enzyme/GA/PANI+HCl or ptoluensulfonic acid/PVC-KTpClPB-o-NPOE connected to a microcomputer (ADI Powerlab instruments, Australia), magnetic stirrer , and flow injection (FIA). PANI dissolved with HCl or p-toluensulfonic acid at the smallest concentration can be dissolved respectively at 6 M and 2 M. Here the electrode is sequentially coated with the first electrode PVA-Enzyme/GA/PANI+HCl/PVC-KTpClPB-o-NPOE, as well as PANI p-toluensulfonate.

Result and Discussion

Results of SEM-EDX Analysis Characterization of PVA-Enzyme-one drop/GA/PANI+HCl 6M/PVC-KTpClPB-o-NPOE

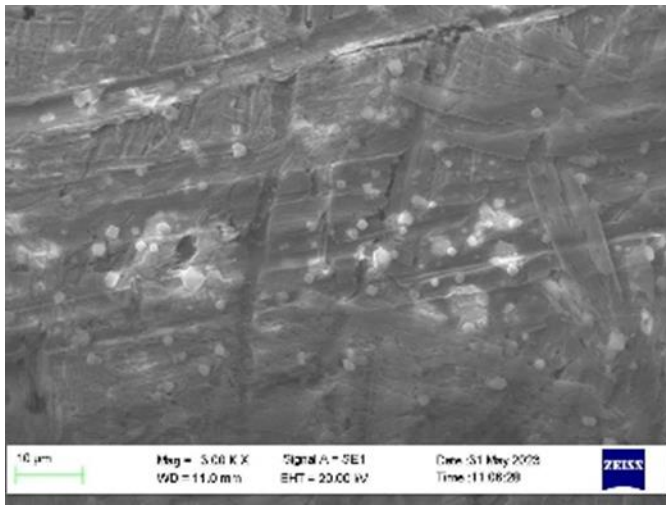

(a)

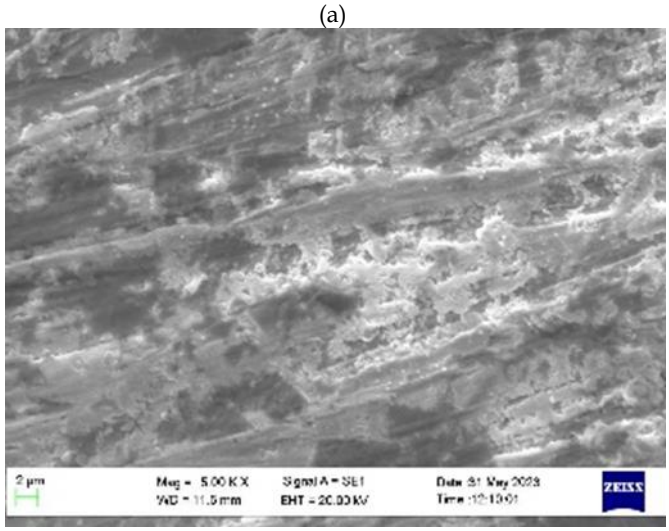

(b)

Figure 1. Morpology of PVA-Enzyme/GA/PANI+HCl 6M/PVC-KTpClPB-o-NPOE, 61% (a) 1 drop, (b) 3 drops

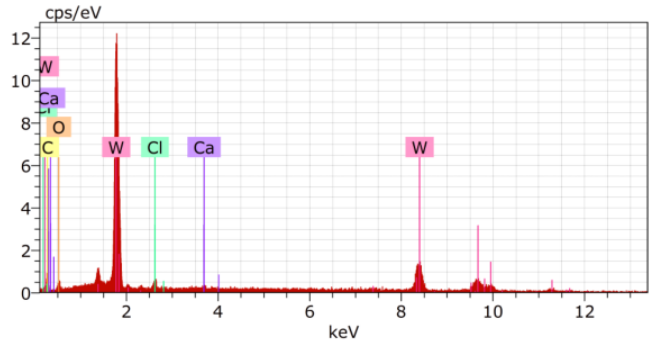

Figure 2. EDX spectrum pattern of PVA-Enzyme-one drop/GA/PANI-HCl 6M/PVC-KTpClPB-o-NPOE-61%

SEM-EDX analysis, Sample 1: PVA-Enzyme 1 drop/GA/PANi-HCl 6M/PVC-KTpClPB-o-NPOE 61% notated S1-Sem-edx; Sample 2: PVA-Enzyme 3 drops/GA/PANi-HCl 6M/PVC-KTpClPB-o-NPOE 61% notation S2-Sem-edx; Sample 3: PVA-Enzyme 1 drop/GA/PANi-p toluene 2M/PVC-KTpClPB-o-NPOE 66% notation S3-Sem-edx; Sample 4: PVA-Enzyme 3 drops/GA/PANi-p toluene 2M/PVC-KTpClPB-o-NPOE 66% notation S4-Sem-edx.

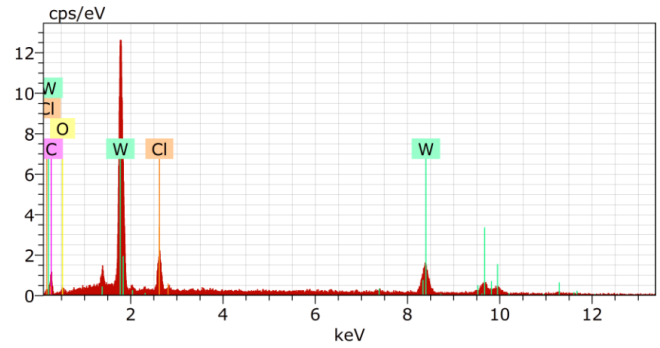

Figure 3. EDX spectrum pattern of PVA-Enzyme-three drops/GA/PANI-HCl 6 M/PVC-KTpClPB-o-NPOE-61%

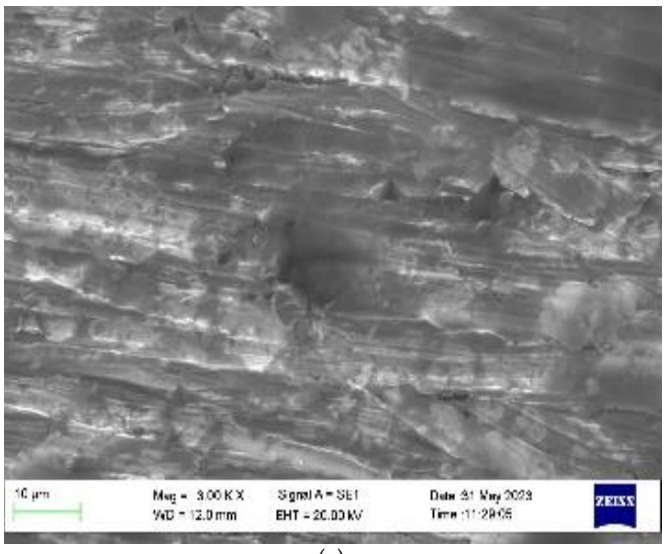

(a)

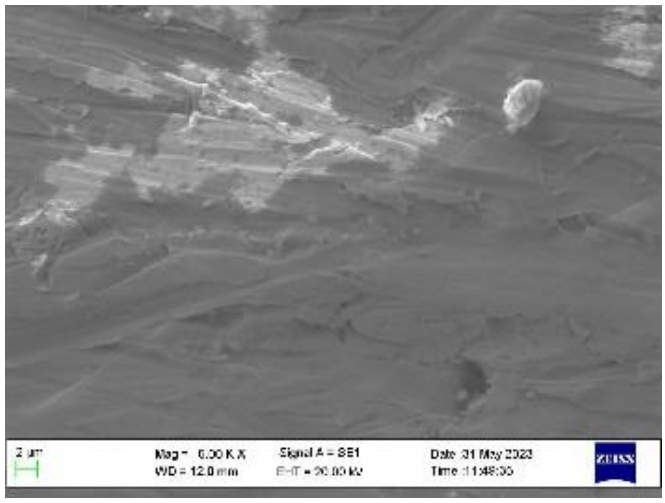

(b)

Figure 4. Morpology of PVA-Enzyme/GA/PANI+p-toluensulfonate 2M/PVC-KTpClPB-o-NPOE, 66%. (a) 1 drop, (b) 3 drops

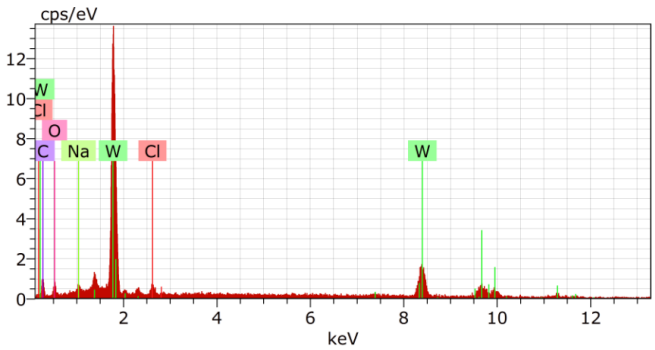

Figure 5. EDX spectrum pattern of PVA-Enzyme-one drop/GA/PANI-p-toluesulfonate 2 M/PVC-KTpClPB-o-NPOE-66%

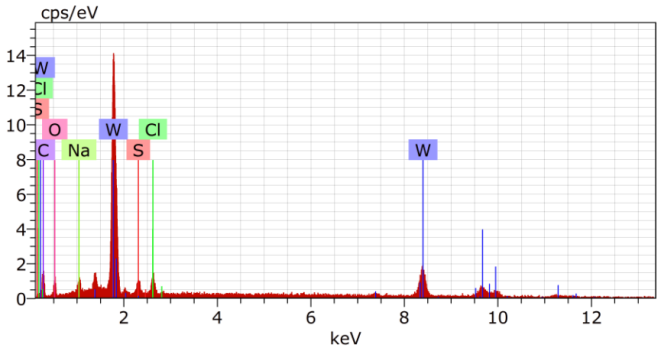

Figure 6. EDX spectrum pattern of PVA-Enzyme-three drops/GA/PANI-p-toluesulfonate 2 M/PVC-KTpClPB-o-NPOE-66%

S1-Sem-edx and S2-Sem-edx have clearer morphological differences (Bohari et al., 2020; Qiu et al., 2020; Tudose et al., 2022; F. Usman et al., 2020) related to pores in S1-Sem-edx figure 1. While the voltage range of S1-Sem-edx is around 12 cps/eV, S2-Sem-edx is greater, namely around 12.25 cps/eV Figures 2 and 3. Show an

increase in the voltage range due to the increase in the number of drops with o-NPOE equal to 61%.

Likewise, there are differences in the morphology of the connected pores of samples S3-Sem-edx and S4-Sem-edx, with larger pores in S3-Sem-edx. The voltage range of the S3-Sem-edx sample is around 12.75 cps/eV, the S4-Sem-edx sample is around 14 cps/eV, indicating an increase due to the number of drops of one drop and three drops of the urease enzyme. Energy dispersive X-ray spectroscopy analysis was carried out to analyze the elemental and chemical composition of the structure (Alipour et al., 2021; Dulgerbaki, 2023; Gamal et al., 2022; Pan et al., 2023; Pani et al., 2016).

Characterization Results of XRD Analysis of PVA-Enzyme/GA/PANI-HCl/PVC-KTpClPB-o-NPOE indicator electrodes

XRD characterization of indicator electrode PVA-Enzyme/GA/PANI-HCl/PVC-KTpClPB-o-NPOE: PVA-E-one drop/GA-2.9%/PANI+HCl/PVC-KTpClPB-oNPOE 61%, sample S2; PVA-E-one drop/GA-2.9%/PANI+HCl/PVC-KTpClPB-oNPOE 66%, sample S5; *PVA-E-three drops/GA*. 9%/PANI+HCl/PVC-KTpClPB-oNPOE 61%, sample S7.

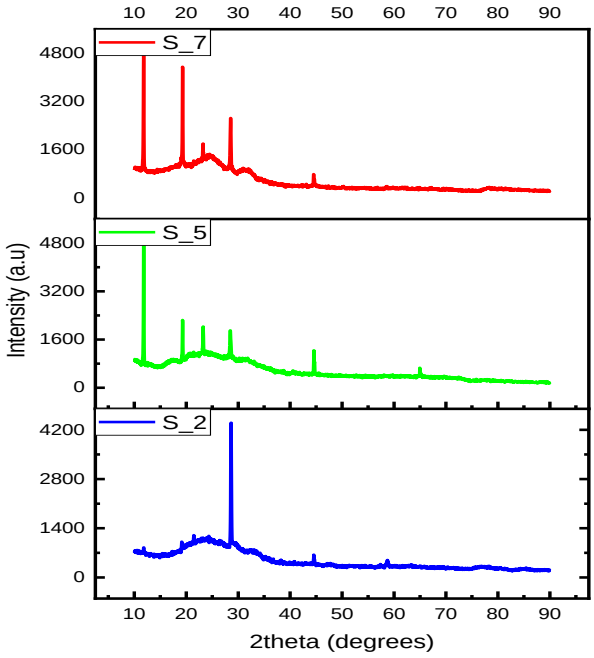

Figure 7. XRD diffraction spectrum pattern of PVA-Enzyme/GA/PANI+HCl 6M/PVC-KTpClPB-o-NPOE indicator electrode (a) one drop of 61% S2, (b) one drop of 66% S5, (c) three drops 61% S7

According to table 1, there are three locations of activity points for the PVA-Enzyme/GA/PANI+HCl 6 M/PVC-KTpClPB-o-NPOE indicator electrode, one drop or three drops of enzyme with variations in o-NPOE of 61% and 66%. According to Figure 7 XRD spectrum pattern (M. Usman et al., 2021) the intensity of 846 a.u of sample S2, 4981 a.u of sample S5, 4888 a.u of sample S7 is around a 2theta diffraction angle of 11.8 degrees. The intensity of 1018 a.u of sample S2, 2249 a.u of sample S5, 4353 a.u of sample S7 is around a diffraction angle of 19 degrees. The intensity of 4400 a.u of sample S2, 1902 a.u of sample S5, 2625 a.u of sample S7 is around a diffraction angle of 28 degrees.

Characterization Results of XRD Analysis of PVA-Enzyme/GA/PANI-p-toluensulfonate/PVC-KTpClPB-o-NPOE indicator electrodes PVC-KTpClPB-oNPOE 61%

Sample S3; PVA-E- one drop/GA-2.9%/PANI+ p-toluensulfonate/PVC-KTpClPB-oNPOE 66%, sample S6; PVA-E-three drops/GA-2.9%/PANI+p-toluensulfonic acid /PVC-KTpClPB-oNPOE 61%, sample S8

Table 1. PVA-Enzyme/GA/PANI+HCl 6 M/PVC-KTpClPB-o-NPOE Indicator Electrode

			Intensity (a.u)
2Theta (degrees)	S2	S5	S7
11.782888159	846.0	4981.0	4888.0
19.135846458	1018.0	1061.0	1406.0
19.293409850	834.0	2249.0	4353.0
28.484607723	1331.0	1902.0	2162.0
28.563389419	3018.0	1616.0	2652.0
28.642171115	4400.0	1386.0	1724.0

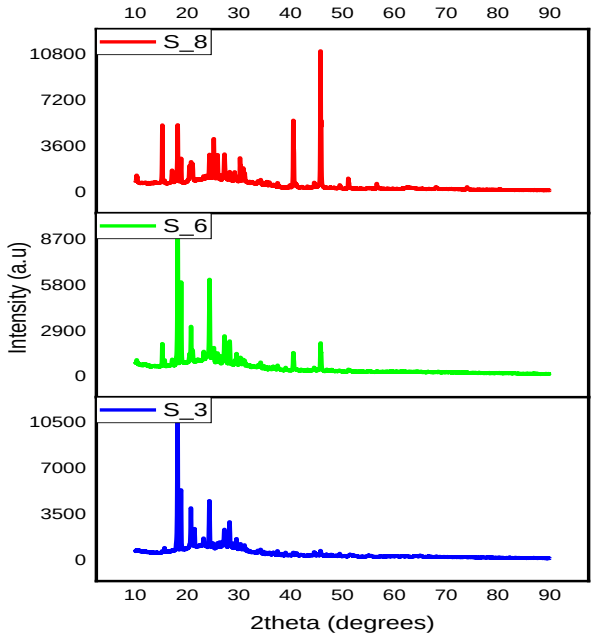

Figure 8. XRD diffraction spectrum pattern of PVA-Enzyme/GA/PANI+p-toluensulfonate 2M/PVC-KTpClPB-o-NPOE indicator electrode (a) one drop of 61% S3, (b) one drop of 66% S6, (c) three drops of 61% S8

According to Figure 8, there is a lot of activity from samples S3, S6, and S8. According to table 2 working points of the XRD spectrum pattern (Beygisangchin et al., 2021; Munaji et al., 2023; M. Usman et al., 2021) the intensity is 10940 a.u for sample S3, 9194 a.u for sample S6, 5312 a.u for sample S8 around the 2theta diffraction angle of 18.1 degrees.

Table 2. PVA-Enzyme/GA/PANI+p-toluensulfonate 2 M/PVC-KTpClPB-o-NPOE Indicator Electrode

2Theta (degrees)	Intensity (a.u)		
	S3	S6	S8
18.164205539	10940.0	8040.0	4855.0
18.190466105	9451.0	9194.0	5312.0

XRD Analysis Characterization Results of PVA-Enzyme/GA/PPy+H2SO4 or PPy+sulfonic acid/PVC-KTpClPB-o-NPOE indicator electrodes

According to Figure 9, the XRD diffraction spectrum pattern of H2SO4-1 intensity is 224 a.u at a 2theta diffraction angle of 44.54 degrees. XRD diffraction spectrum pattern of H2SO4-3 intensity 236 a.u at 2theta diffraction angle 44.48 degrees. XRD diffraction spectrum pattern of AS-1204 a.u intensity at a diffraction angle of 2theta 44.54 degrees. XRD diffraction spectrum pattern of AS-3 intensity 228 a.u at 2theta diffraction angle 44.5 degrees. According to the analysis of figure 7 PANI+HCl 6M and figure 8 PANI+p-toluensulfonate 2M and the properties of p-toluensulfonic acid are stronger than hydrochloric acid HCl. The intensity of PANI+p-toluensulfonate 2M is two times greater than PANI+HCl 6M. Likewise, according to Figure 9, the intensity of PPy+H2SO4 8M is greater than the intensity of PPy+sulfonic acid 2M (Martínez-Cartagena, 2022; Arslantürk & Ugraskan, 2023).

Based on Figures 7, 8 and Figure 9, the intensity shows that the intensity of the strong acid is large and the PPy conducting polymer is smaller than PANI and the intensity of PPy is smaller than PANI.

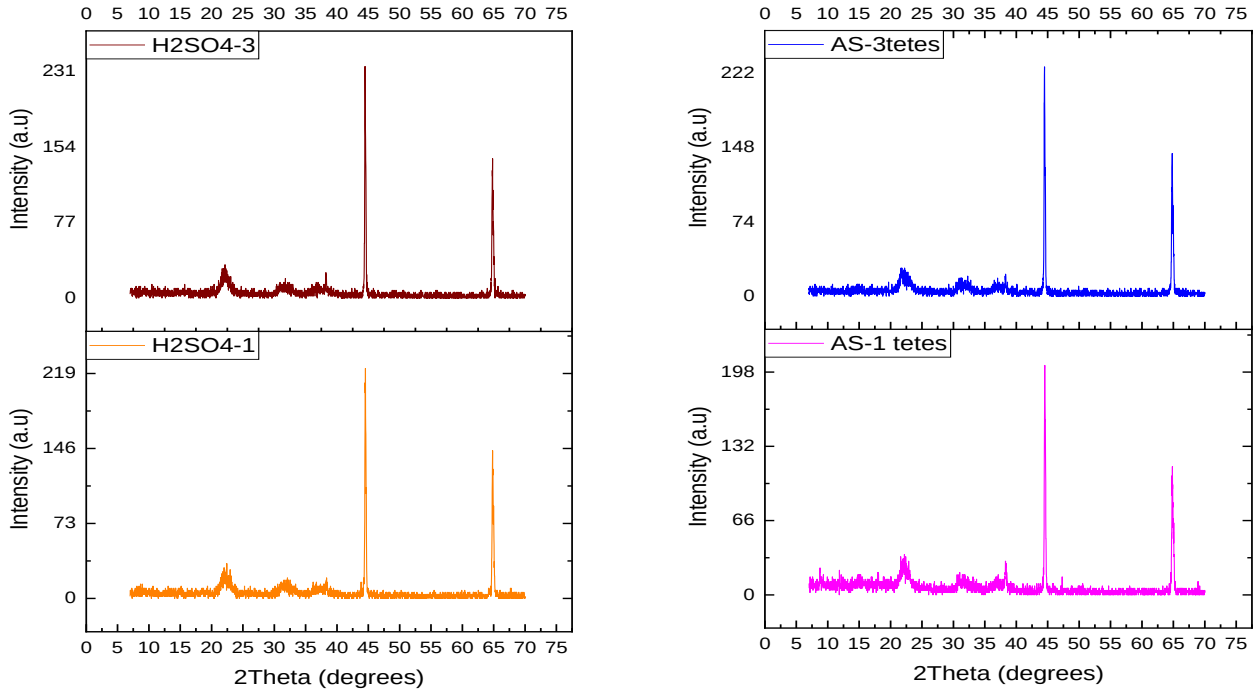

Figure 9. XRD diffraction spectrum pattern of PVA-Enzyme/GA/PPy+H2SO4 8M indicator electrode, PPy+2M sulfonic acid /PVC-KTpClPB-o-NPOE

Table 3. Indicator electrodes (a) H_2SO_4-1, (b) H_2SO_4-3, (c) AS-1, (d) AS-3

2Theta (degrees)	H_2SO_4-1	H_2SO_4-3	AS-1	AS-3
44.48	166	236	140	220
44.5	210	216	164	228
44.54	224	172	204	176

FTIR Characterization Results of PVA-Enzyme/GA/PPy+ H2SO4 or PANI+HCl /PVC-KTpClPB-o-NPOE indicator electrodes

According to Figure 9, the FTIR spectrum pattern decreases in transmittance between wave numbers 3500 - 500 cm^{-1} (Katowah et al., 2021) for the PVA-Enzyme-one drop/GA/PPy+H2SO4 /PVC-KTpClPB-o-NPOE indicator electrode (Hakim S, 2023).

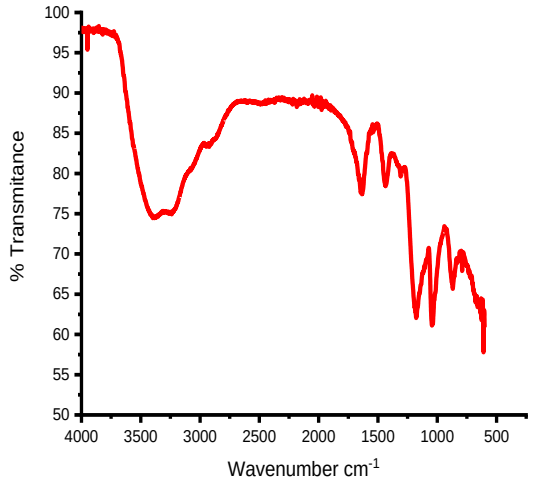

Figure 9. FTIR transmittance spectrum pattern of the PVA-Enzyme-one drop/GA/PPy+H2SO4 /PVC-KTpClPB-o-NPOE indicator electrode

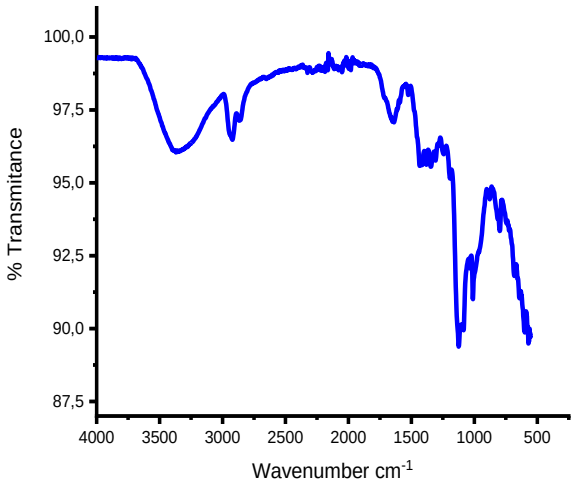

Figure 10. FTIR transmittance spectrum pattern of the indicator electrode PVA-Enzyme-one drop/GA/PANI+HCl /PVC-KTpClPB-o-NPOE 61%

According to Figure 10, the FTIR spectrum pattern increases in transmittance between wave numbers 3500 - 500 cm^{-1} (Aizamddin et al., 2022; Bohari et al., 2020; Guerrero et al., 2018; Katowah et al., 2021; Yao et al., 2019) for the indicator electrode PVA-Enzyme-one drop/GA/ PANI+HCl /PVC-KTpClPB-o-NPOE 61% . The increase in transmittance properties is related to the polymer conduction properties of PANI being greater than the conduction properties of PPy. The rate capability of conductive hydrogels decreased in the order of polypyrrole (PPy) > polyaniline (PANI) > poly(acrylic acid) (PAA) (Alipour et al., 2021; Gao et al., 2019; Li, 2017; Nawaz et al., 2014).

Conclusion

Based on the data above, SEM-EDX analysis determines the membrane pore morphology and EDX determines the voltage range in cps/eV which increases with the number of drops of urease and o-NPOE plasticizer enzymes. XRD analysis determined that the acidic properties and conduction properties of PANI polymer were stronger than PPy. FTIR analysis determines the transmittance properties, meaning the conductivity properties of the polymer.

Acknowledgments
Thanks to all parties who have supported the implementation of this research. I hope this research can be useful.

Author Contributions
Conceptualization, methodology, validation, formal analysis, investigation, resources, data curation, writing—original draft preparation, writing—review and editing, visualization: Abd Hakim S[1].

Funding
This research was independently funded by researchers.

Conflicts of Interest
The authors declare no conflict of interest.

References

Aizamddin, M. F., Mahat, M. M., Zainal Ariffin, Z., Nawawi, M. A., Jani, N. A., Nor Amdan, N. A., & Sadasivuni, K. K. (2022). Antibacterial Performance of Protonated Polyaniline-Integrated Polyester Fabrics. *Polymers*, *14*(13), 2617. https://doi.org/10.3390/polym14132617

Alipour, A., Mansour Lakouraj, M., & Tashakkorian, H. (2021). Study of the effect of band gap and photoluminescence on biological properties of polyaniline/CdS QD nanocomposites based on natural polymer. *Scientific Reports*, *11*(1), 1913. https://doi.org/10.1038/s41598-020-80038-1

Beygisangchin, M., Abdul Rashid, S., Shafie, S., & Sadrolhosseini, A. R. (2021). Polyaniline Synthesized by Different Dopants for Fluorene Detection via Photoluminescence Spectroscopy. *Materials*, *14*(23), 7382. https://doi.org/10.3390/ma14237382

Bohari, N. A., Siddiquee, S., Saallah, S., Misson, M., & Arshad, S. E. (2020). Optimization and Analytical Behavior of Electrochemical Sensors Based on the Modification of Indium Tin Oxide (ITO) Using PANI/MWCNTs/AuNPs for Mercury Detection. *Sensors*, *20*(22), 6502. https://doi.org/10.3390/s20226502

Dulgerbaki, C. (2023). Development of Poly(2-Methyl

Thioaniline)/Vanadium Pentoxide Hybrid Electrode Material for High Performance Supercapacitor Applications. *Journal of Macromolecular Science, Part B*, *62*(9), 504–513. https://doi.org/10.1080/00222348.2023.2232250

Elbehery, N. H. A., Amr, A. E.-G. E., Kamel, A. H., Elsayed, E. A., & Hassan, S. S. M. (2019). Novel Potentiometric 2,6-Dichlorophenolindo-phenolate (DCPIP) Membrane-Based Sensors: Assessment of Their Input in the Determination of Total Phenolics and Ascorbic Acid in Beverages. *Sensors*, *19*(9), 2058. https://doi.org/10.3390/s19092058

Gamal, A., Shaban, M., BinSabt, M., Moussa, M., Ahmed, A. M., Rabia, M., & Hamdy, H. (2022). Facile Fabrication of Polyaniline/Pbs Nanocomposite for High-Performance Supercapacitor Application. *Nanomaterials*, *12*(5), 817. https://doi.org/10.3390/nano12050817

Gao, H., Cai, M., & Liao, Y. (2019). Enhance photocatalytic properties of TiO 2 using π-π* conjugate system. *Journal of Dispersion Science and Technology*, *40*(10), 1469–1478. https://doi.org/10.1080/01932691.2018.1518143

Guerrero, J., Carrillo, A., Mota, M., Ambrosio, R., & Aguirre, F. (2018). Purification and Glutaraldehyde Activation Study on HCl-Doped PVA–PANI Copolymers with Different Aniline Concentrations. *Molecules*, *24*(1), 63. https://doi.org/10.3390/molecules24010063

Hakim S, A. (2022). Characterization of PVA-Enzyme Coated Indicator Electrodes GA coated again with PVC-KTpClPB-o-NPOE SEM-EDS, FTIR and XRD analysis. *Jurnal Penelitian Pendidikan IPA*, *8*(1), 103–108. https://doi.org/10.29303/jppipa.v8i1.1265

Hakim S, A. (2023). Synthesis and Characterization of PVA-Enzyme/GA/PPy/ PVC-KTpClPB-o-NPOE Indicator Electrodes, XRD Analysis, FTIR and Variable Signal Analysis. *Jurnal Penelitian Pendidikan IPA*, *9*(3), 1149–1154. https://doi.org/10.29303/jppipa.v9i3.2389

Hsu, P.-Y., Hu, T.-Y., Kumar, S., Wu, K., & Lue, S. (2022). Swelling-Resistant, Crosslinked Polyvinyl Alcohol Membranes with High ZIF-8 Nanofiller Loadings as Effective Solid Electrolytes for Alkaline Fuel Cells. *Nanomaterials*, *12*(5), 865. https://doi.org/10.3390/nano12050865

Katowah, D. F., Saleh, S. M., Alqarni, S. A., Ali, R., Mohammed, G. I., & Hussein, M. A. (2021). Network structure-based decorated CPA@CuO hybrid nanocomposite for methyl orange environmental remediation. *Scientific Reports*, *11*(1), 5056. https://doi.org/10.1038/s41598-021-84540-y

Kaur, H., Chhibber, M., & Mittal, S. (2017). Acyclic Arylamine-Based Ionophores as Potentiometric Sensors for Zn2+ and Ni2+ Ions. *C*, *3*(4), 34. https://doi.org/10.3390/c3040034

Li, C. (2017). *Advanced Nanomaterials for Renewable Energy and Sustainability, The Dissertation of Changling Li is approved*. University of California Riverside.

Munaji, Zainuri, M., & Triwikantoro. (2023). Structures and electric properties of PANI/polymorphic-ZrO 2 composites. *RSC Advances*, *13*(15), 10414–10423. https://doi.org/10.1039/D3RA01088K

Nawaz, S., Siddiq, M., Kausar, A., Hussain, S. T., & Abbas, F. (2014). Facile Synthesis and Properties of Multilayered Polyaniline/Polypyrrole/Epoxy/Polystyrene/Fu nctionalized Carbon Nanotube Composites. *Polymer-Plastics Technology and Engineering*, *53*(7), 661–670. https://doi.org/10.1080/03602559.2013.874032

Pan, Y., Hu, S., Zheng, X., Hu, N., Qiu, F., Dai, M., Guo, Q., Yu, X., Hao, Y., Lv, M., & Huang, J. (2023). Efficient electromagnetic interference shielding of three-dimensional hydrophobic Cu/wood/Cu porous composites. *Journal of Wood Chemistry and Technology*, *43*(4), 206–220. https://doi.org/10.1080/02773813.2023.2213691

Pani, A., Lee, J. H., & Yun, S. I. (2016). Autoclave mediated one-pot-one-minute synthesis of AgNPs and Au-Ag nanocomposite from Melia azedarach bark extract with antimicrobial activity against food pathogens. *Chemistry Central Journal*, *10*(1). https://doi.org/10.1186/s13065-016-0157-0

Qiu, B., Wang, J., Li, Z., Wang, X., & Li, X. (2020). Influence of Acidity and Oxidant Concentration on the Nanostructures and Electrochemical Performance of Polyaniline during Fast Microwave-Assisted Chemical Polymerization. *Polymers*, *12*(2), 310. https://doi.org/10.3390/polym12020310

Terán-Alcocer, Á., Bravo-Plascencia, F., Cevallos-Morillo, C., & Palma-Cando, A. (2021). Electrochemical Sensors Based on Conducting Polymers for the Aqueous Detection of Biologically Relevant Molecules. *Nanomaterials*, *11*(1), 252. https://doi.org/10.3390/nano11010252

Tudose, I. V., Mouratis, K., Ionescu, O. N., Romanitan, C., Pachiu, C., Popescu, M., Khomenko, V., Butenko, O., Chernysh, O., Kenanakis, G., Barsukov, V. Z., Suchea, M. P., & Koudoumas, E. (2022). Novel Water-Based Paints for Composite Materials Used in Electromagnetic Shielding Applications. *Nanomaterials*, *12*(3), 487. https://doi.org/10.3390/nano12030487

Usman, F., Dennis, J. O., Meriaudeau, F., Ahmed, A. Y., Seong, K. C., Fen, Y. W., Sadrolhosseini, A. R., Abdulkadir, B. A., Ayinla, R. T., Daniyal, W. M. E. M. M., Omar, N. A. S., Tamam, N., & Sulieman, A.

(2020). Dependence of the Optical Constant Parameters of p-Toluene Sulfonic Acid-Doped Polyaniline and Its Composites on Dispersion Solvents. *Molecules*, *25*(19), 4414. https://doi.org/10.3390/molecules25194414

Usman, M., Adnan, M., Ahsan, M. T., Javed, S., Butt, M. S., & Akram, M. A. (2021). In Situ Synthesis of a Polyaniline/ Fe-Ni Codoped Co3O4Composite for the Electrode Material of Supercapacitors with Improved Cyclic Stability. *ACS Omega*, *6*(2), 1190–1196. https://doi.org/10.1021/acsomega.0c04306

Vlascici, D., Cosma, E. F., Pica, E. M., Cosma, V., Bizerea, O., Mihailescu, G., & Olenic, L. (2008). Free base porphyrins as ionophores for heavy metal sensors. *Sensors*, *8*(8), 4995–5004. https://doi.org/10.3390/s8084995

Yao, J., Chen, Y., Li, W., Chen, X., & Fan, X. (2019). Fabrication and characterization of electrospun PLLA/PANI/TSA fibers. *RSC Advances*, *9*(10), 5610–5619. https://doi.org/10.1039/C8RA10495F